Investigation of Superluminescent Diodes for Smart-Lighting Systems

Ashwin K. Rishinaramangalam, Arman Rashidi, Morteza Monavarian, Andrew A. Aragon, Saadat Mishkat Ul Masabih, and Daniel F. Feezell

University of New Mexico, Albuquerque, NM - 87131

Motivation

Applications of visible SLDs

Automotive lighting (Droop-free)

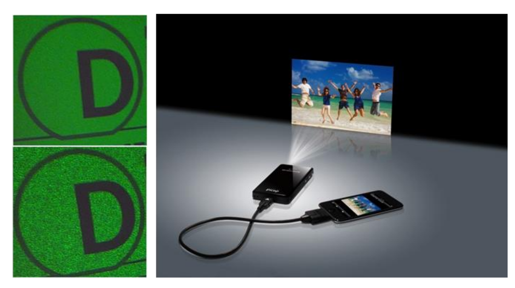

Pico-projection (Speckle-free)

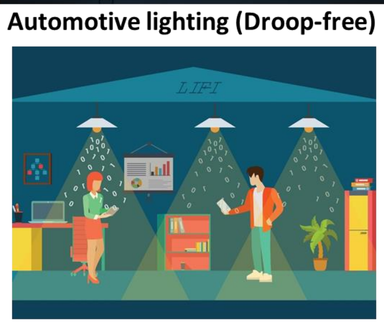

Visible-light Communication (VLC) (High modulation bandwidth)

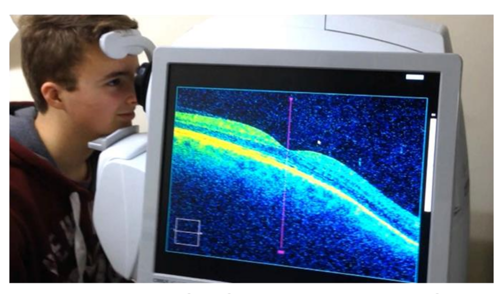

Optical Coherence Tomography (High resolution imaging)

Advantages of SLDs over LEDs and Lasers

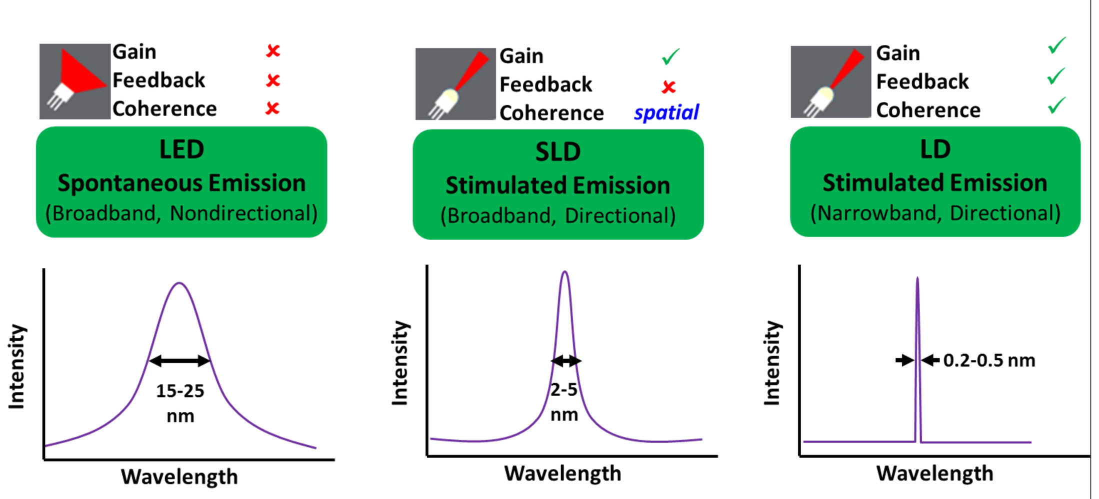

Radiative Efficiency

LED	Laser Above Threshold
$\eta_r = \frac{BN^2}{AN + BN^2 + CN^3}$	$\eta_r = \frac{BN_{th}^2 + R_{st}}{AN_{th} + BN_{th}^2 + CN_{th}^3 + R_{st}}$
Depends on carrier density → droop	Independent of carrier density → no droop

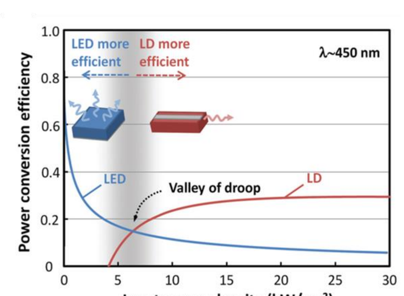

Comparison of the expression for IQE using the ABC model for spontaneous emission dominated devices (LEDs) and stimulated emission dominated devices (SLDs and laser diodes)[J. J. Wierer et al., (2013)]

Advantages of nonpolar SLDs over c-plane SLDs

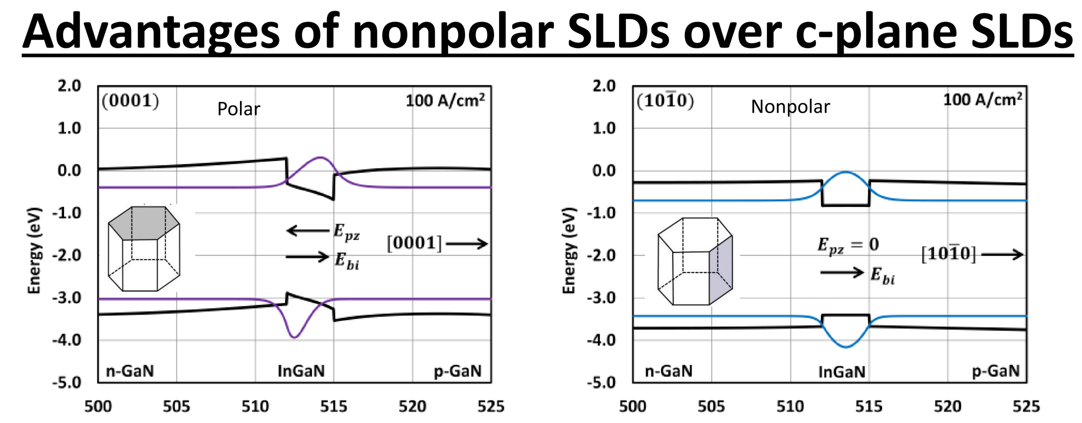

Energy band simulations of polar and nonpolar active regions[1] at 100 A/cm²

✓ Higher radiative efficiency ✓ Lower blueshift ✓ Shorter carrier lifetime (larger modulation BW)
✓ Allows thicker QWs (higher confinement, lower droop, AlGaN-cladding-free)

Higher gain in m-plane active regions

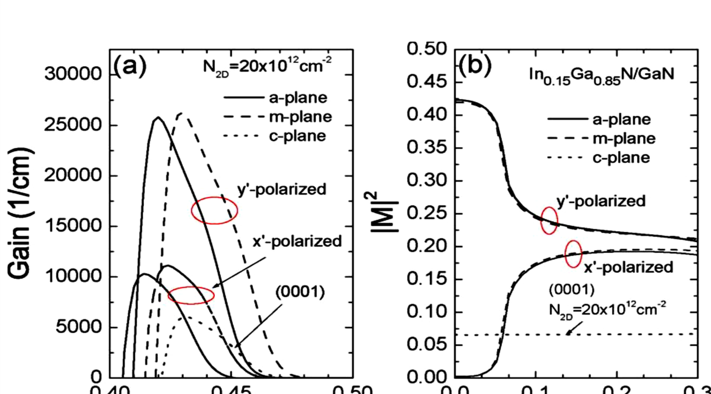

$P_{out} \approx P_{SP} \exp[(\Gamma g - \alpha_i)L]$

- ✓ Higher output power
- ✓ Higher differential efficiency
- ✓ Higher modulation bandwidth

Gain and wavefuntion overlap of c-plane, m-plane and a-plane active regions versus emission wavelength[2]

[1] D. F. Feezell et al., J. of Displ. Technol. 9, 190 (2013)
[2] Park et al., IEEE Journal Of Quantum Electronics, 43, 12, (2007)

SLD Epitaxial Growth and Fabrication

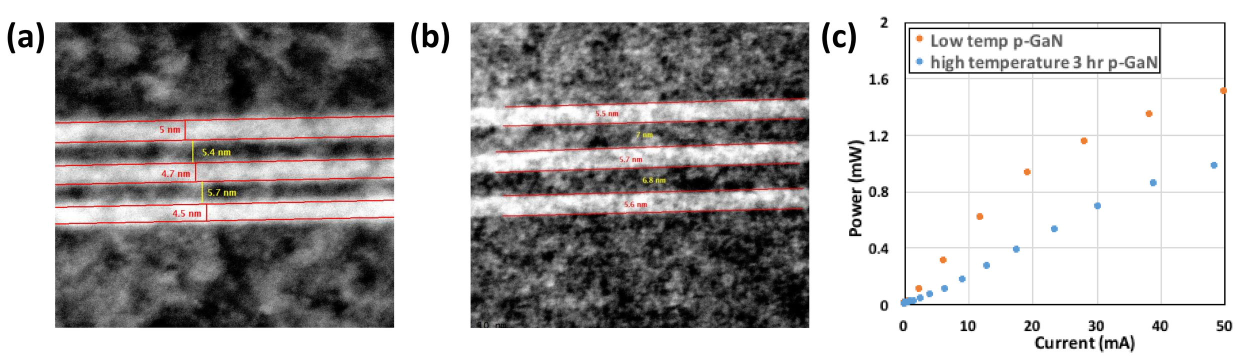

Comparison of active region area of planar *m*-plane LEDs with (a) 3 hr long p-GaN growth and (b) 45 min long p-GaN growth. The active region quality is improved considerably in the shorter p-GaN growth, confirmed by improved optical output power at a given current (c).

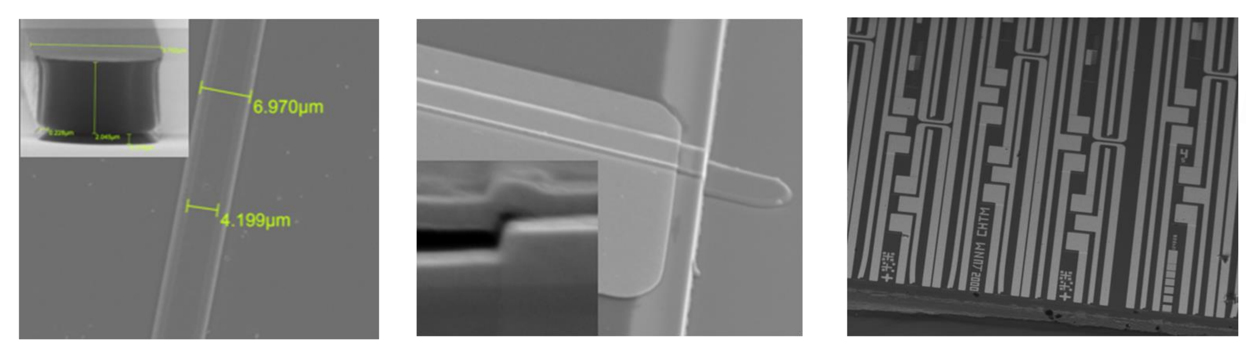

Self-aligned SiO_2 deposition. Inset shows the bilayer resist pattern used for achieving self-aligned dielectric

Facet-etch indicating good quality facets. Inset shows cross-section at the ridge

Fabricated SLD and laser arrays with pads for RF testing

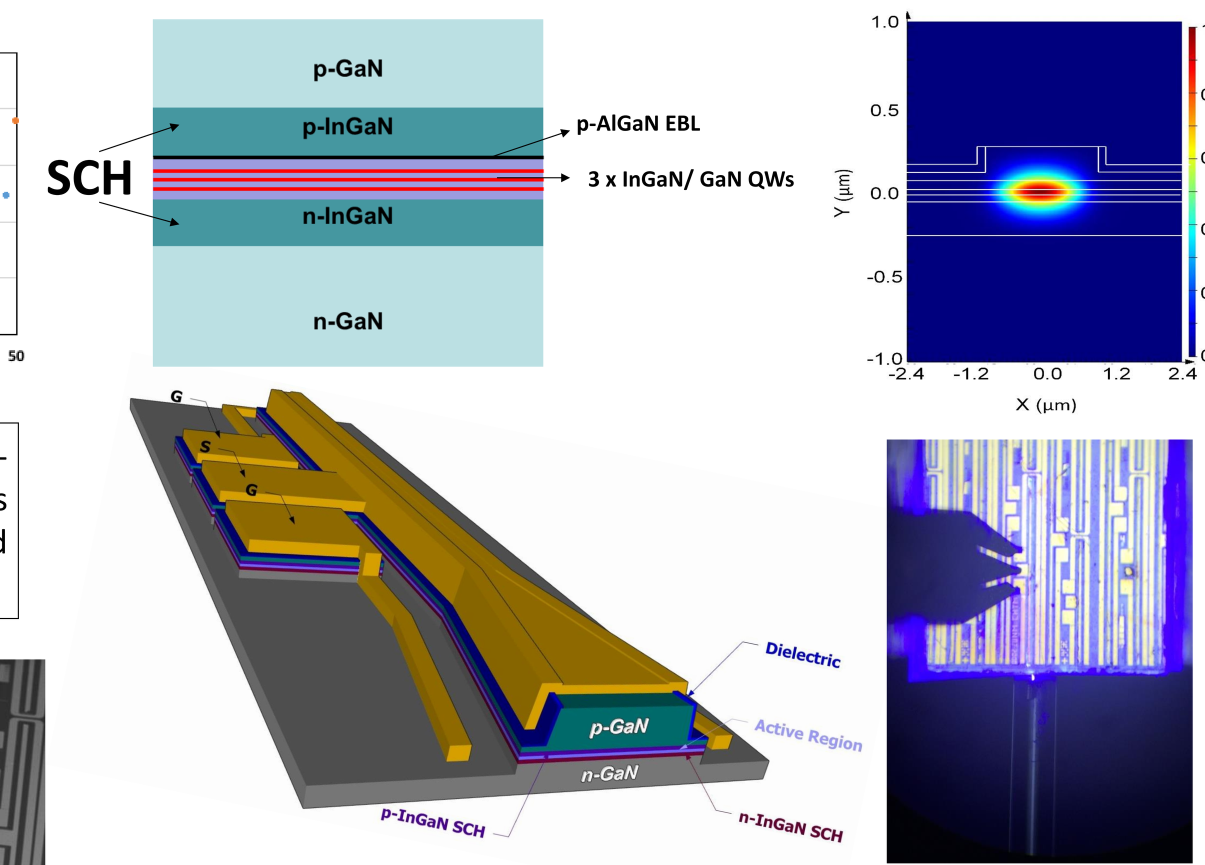

(a) Epitaxial layer structure of the SLD indicating the separately-confined heterostructure guiding, whose simulated mode profile using Lumerical (FDTD) is shown in (b). (c) Pictographic illustration of a fabricated tapered waveguide SLD (TSLD). (d) A TSLD under electrical operation

Electrical, Optical, and RF Characterization

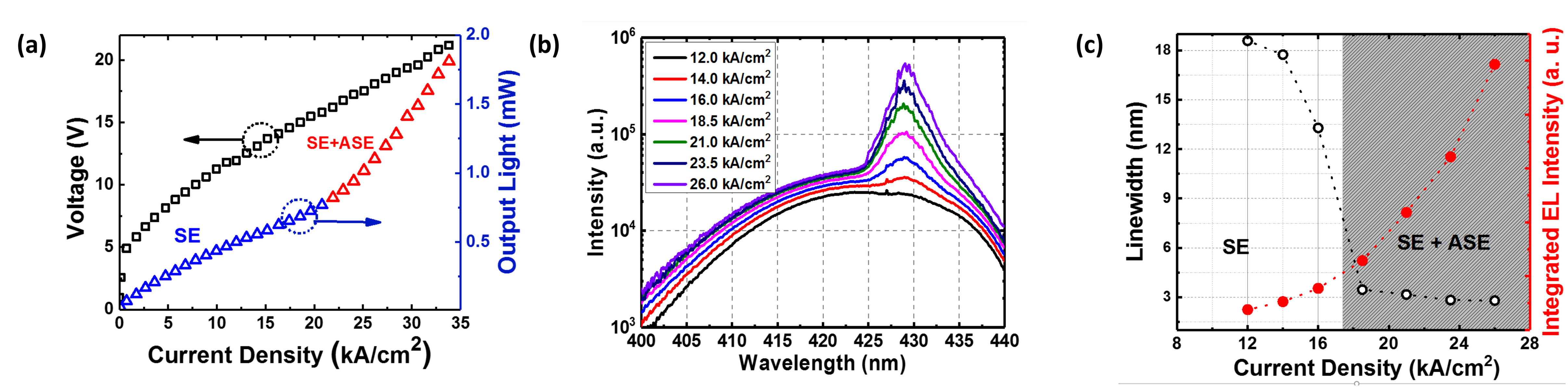

(a) L-J-V characteristics of TSLD. Spectral evolution is shown in (b). (c) Linewidth and total integrated power of the EL spectrum versus current density.

$$f_{3dB} \approx \frac{1.55}{2\pi}\sqrt{\frac{\Gamma^2 v_g^2\, a(\alpha_m+\alpha_i)\beta(J-J_{tr})}{\alpha_m V}}\, exp[\frac{(\Gamma\beta(J-J_{tr})-\alpha_i)L}{2}]$$

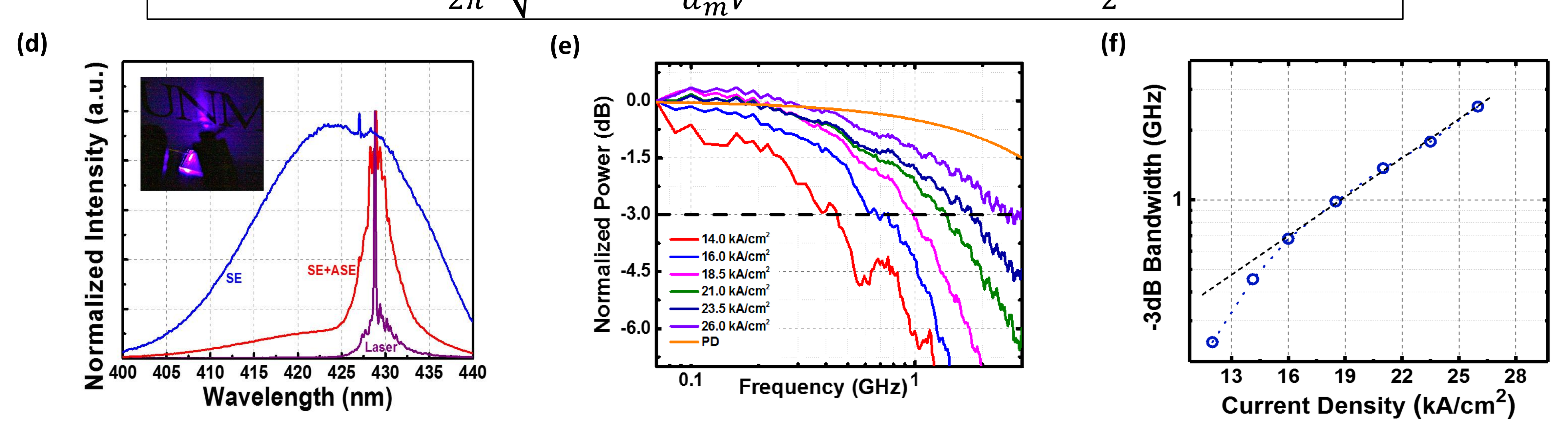

(d) Normalized EL spectra of LED, SLD, and laser on the same chip. (e) Frequency response of the TSLD. The -3 dB RF modulation bandwidth is obtained and plotted versus current density in (f). The log(f_{3dB}) goes linearly as a function of J in the superluminescene regime due to the exponential increase of the o/p power with J, evident from the above equation.

Record Modulation Bandwidth of Blue Micro-LEDs

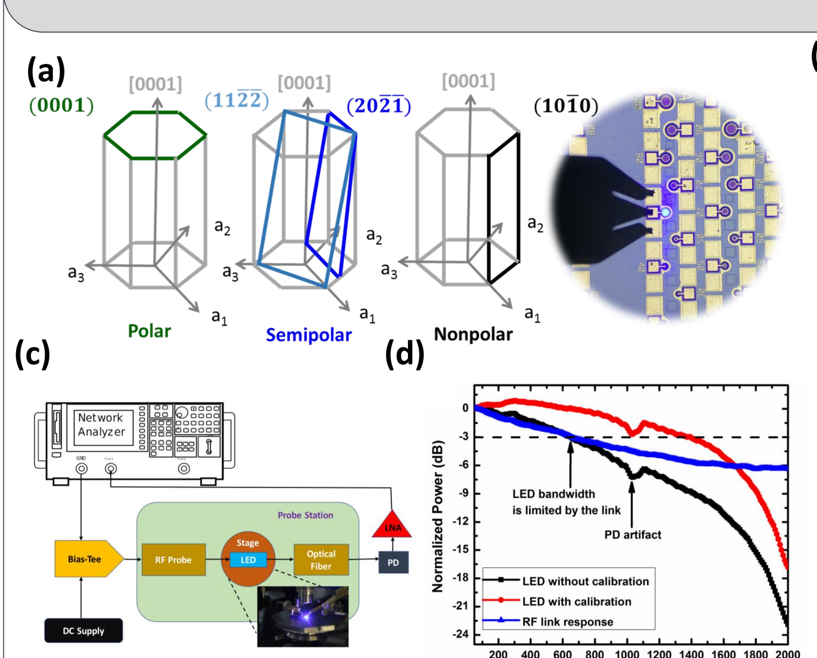

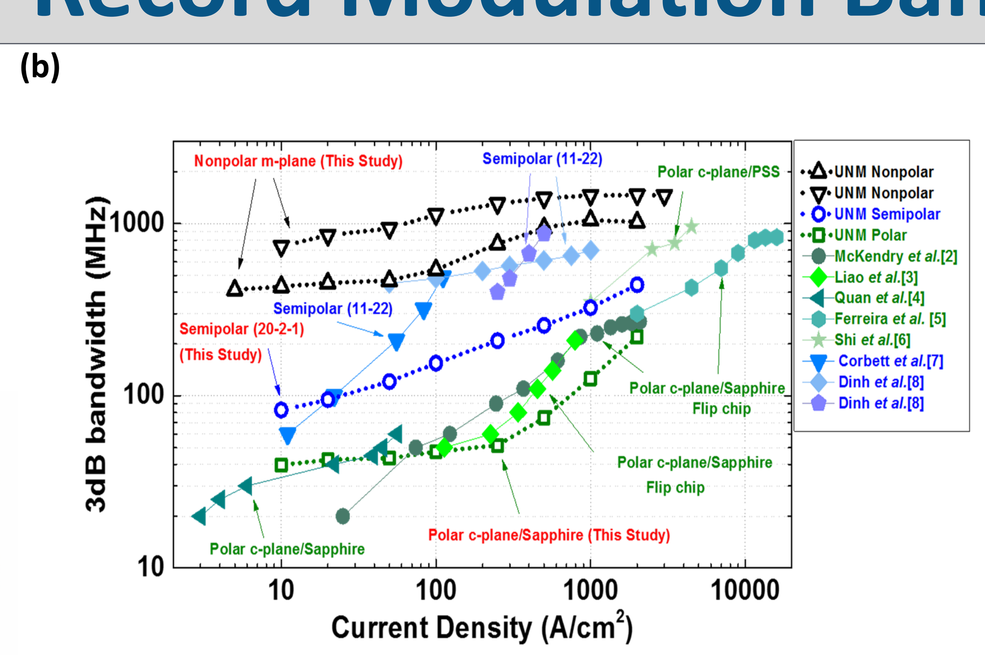

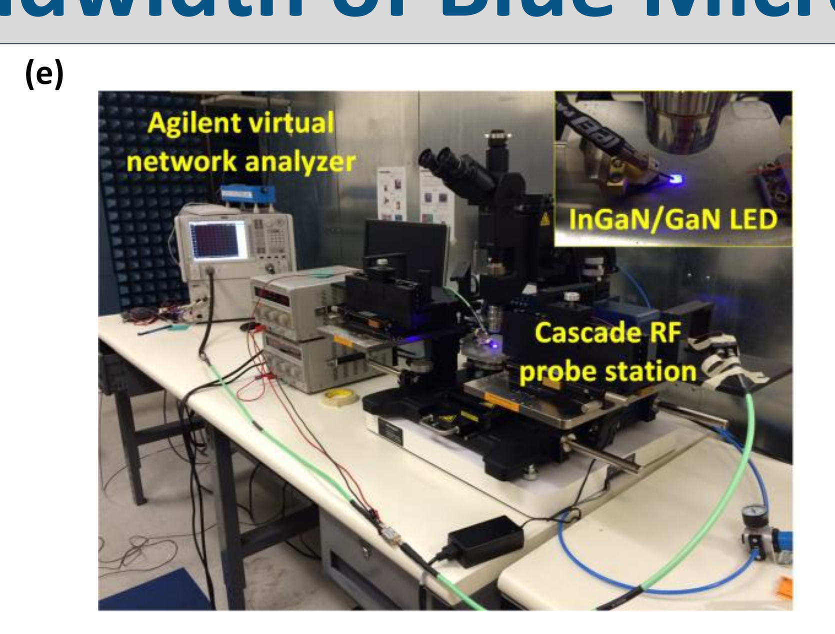

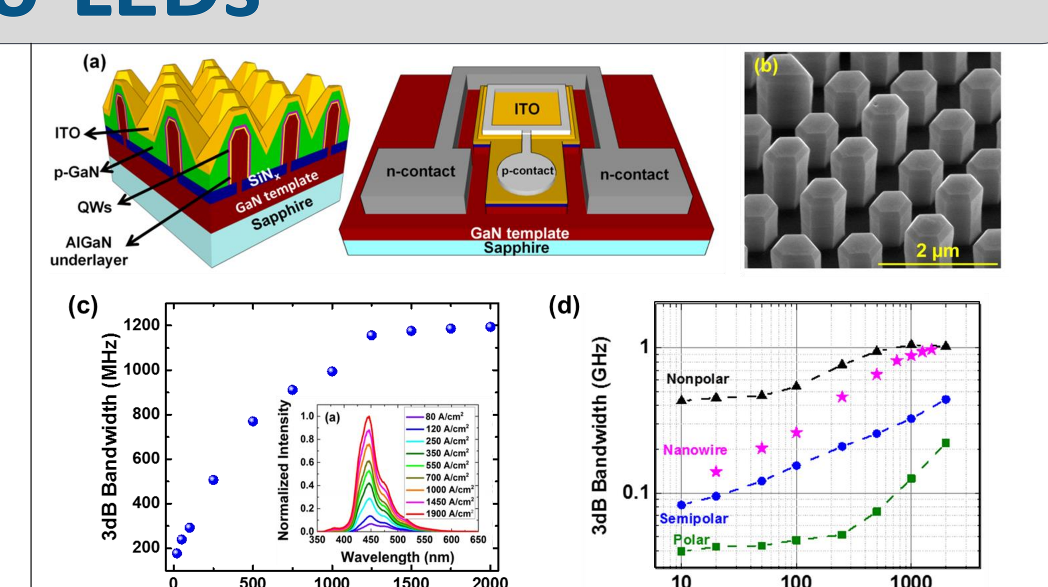

(a) Schematic illustration of the various crystallographic planes analyzed; The inset shows an LED device probed using a GSG RF probe. (b) Bandwidth vs. current density for the nonpolar, semipolar, and conventional *c*-plane microLEDs, compared to other reported *c*-plane LEDs on sapphire and semipolar substrates. *c*-plane data from Refs. [2-6] and semipolar data from Refs. [7-8]. (c) RF setup for measuring the frequency response of the LED. (d) Effect of calibration of the RF link on the frequency response of the LED. (e) Test station for SLD bandwidth characterization. Inset shows an InGaN/GaN LED under test.

(a) Illustration of a nanowire-based micro-LED on sapphire. (b) Arrays of GaN nanowires indicative of smooth morphology on the *m*-plane sidewalls. (c) -3dB bandwidth of the nanowire LED as a function of current density. Inset image shows the EL spectra progression for different current densities. (d) Comparison of the -3dB bandwidth for micro-LEDs on different orientations.

LESA Lighting Enabled Systems & Applications

New Mexico EPSCoR